Journal of Geoscience and Environment Protection, 2026, 14(2), 1-18
https://www.scirp.org/journal/gep
ISSN Online: 2327-4344
ISSN Print: 2327-4336

Analysis of Lineaments for Identifying Potential Subsidence Zones in Conakry: The Case of the Former Municipality of Ratoma (Guinea)

Ninamou Tökpö[1,2,3], Kolié Labilé[2], Elégbédé Manou Bernadin[1]

[1]Laboratory of Science and Technology of Water and the Environment (LSTEE), National Institute of Water (INE), African Centre of Excellence for Water and Sanitation (C2EA), University of Abomey-Calavi (UAC), Cotonou, Benin
[2]Department of Civil Engineering, Gamal Abdel Nasser University of Conakry, Conakry, Republic of Guinea
[3]Hydraulics Laboratory of the Small Hydropower Technology Center, Gamal Abdel Nasser University of Conakry, Conakry, Guinea
Email: cecedavid2015@gmail.com

How to cite this paper: Tökpö, N., Labilé, K., & Bernadin, E. M. (2026). Analysis of Lineaments for Identifying Potential Subsidence Zones in Conakry: The Case of the Former Municipality of Ratoma (Guinea). *Journal of Geoscience and Environment Protection, 14,* 1-18.
https://doi.org/10.4236/gep.2026.142001

Received: December 24, 2025
Accepted: January 27, 2026
Published: January 30, 2026

Abstract

Ratom was one of the five communes of Conakry (Guinea) before the administrative division of 2025. It faces risks of soil subsidence. To identify areas susceptible to subsidence or collapse, lineament analysis was used to locate areas with low mechanical resistance. This study proposes a multidisciplinary methodological approach to assess and map subsidence risks in the study area. It combines remote sensing techniques, geostatistical analysis, geotechnical methods, and multicriteria decision-making methods. Automatic extraction of lineaments from a Landsat 8 image identified 1011 lineaments. Analysis reveals that 68% of these are minor lineaments, while 12% are major lineaments. This may reflect geological discontinuities that impact soil stability. After validation by comparison with the road and hydrographic networks, these lineaments were analyzed using a variogram model to produce a map of risk areas. At the same time, data from geotechnical tests on 11 samples were used to measure paramters such as water content, grain size, and Atterberg limits. The liquidity index (LI) proved to be a determining factor in assessing the risk of subsidence. In addition, a multi-criteria approach using the AHP method took five factors into account: fracture density, mechanical strength, liquidity index, slope, and altitude. The map obtained from this analysis shows that 49.06% of the surface area of Ratoma is exposed to a high risk of subsidence. Critical areas such as Kobaya, Kiroti, and the Kakimbo-University axis, which often experience sub-

sidence, are well located within the identified risk areas. This approach has made it possible to produce a tool for sustainable urban planning and risk prevention in this municipality.

Keywords

Ratoma, Remote Sensing, Lineament, AHP Method, Risk of Subsidence

1. Introduction

The municipality of Ratoma faces growing geological and urban challenges, including the risk of subsidence. This municipality was recently divided into three urban municipalities (Ratoma, Lambanyi, and Sonfonia) (Doré, 2024). It is characterized by a humid tropical climate, with an average temperature of 27.3˚C and annual rainfall of around 1430 mm, which promotes soil weathering. Ratoma has an expanding urban landscape. Log data from the forages reveal a complex geology, where lineaments could reveal areas of potential subsidence.

Research conducted by Ninamou & Diakité (2021) identified 1090 operational boreholes, covering 25 of the 32 districts in the study area. However, a hydraulic drilling campaign carried out in 2009 as part of a presidential emergency initiative in Conakry yielded less encouraging results. Of the 180 wells drilled, 18 are unproductive, representing a failure rate of 10%. Sixteen of the unproductive wells are located in Ratoma, accounting for 90% of the total failures and 20% of the wells drilled in this municipality (SEG, 2009). These failures are mainly due to the lack of preliminary studies to locate exploitable reservoirs. The objective of the "Water for All" project was to supply water to the population through local boreholes by drilling 150 boreholes in Greater Conakry.

Furthermore, since the commissioning of the Kobaya and Nongo Stade catchment fields in 2004 and 2013, respectively, persistent cracks have been observed in the surrounding soil and buildings. These geotechnical problems could be attributed to subsidence or hydrogeological changes caused by intensive groundwater extraction, highlighting the urgent need for enhanced monitoring of the environmental impacts associated with water resource exploitation.

The identification of lineaments using remote sensing techniques (via color compositions) and GIS (LINE tool via Geomatica's Librarian algorithm), and their validation in the field by comparison with road and hydrographic networks and drilling data are commonly used techniques (Oludayo et al., 2021; Yoshe, 2023; Matar et al., 2023; Fuladi & Deshmukh, 2021; Kamaraj et al., 2023a; Embaby et al., 2024). This technique, combined with the geotechnical results obtained at the Conakry Geoscience Agency laboratory, makes it possible to assess geotechnical risks and identify risk areas. This strategy is an innovative contribution to the identification of geotechnical risk areas. The approach, inspired by the work of Jourda (2005), which uses spatial and geostatistical data

combined with geotechnical data to map risk areas, is essential for responsible and sustainable development in Ratoma.

2. Materials-Data-Methods

2.1. Materials-Data

For this study, we used geological and geophysical maps of Guinea at a scale of 1:500,000 produced by Galperov G., combined with GPS surveys. ArcGIS was used for satellite image processing (Landsat 8 OLI/TIRS image from January 29, 2025, downloaded from USGS at https://earthexplorer.usgs.gov/; the sky was clear during this period). Geomatica and RockWorks 17 software were used to extract the lineaments, and Google Earth Pro was used to delimit the study area. The drilling data comes from institutional sources (SEG, SNAPE, UNICEF) and private drilling operations. These data enable a comprehensive analysis of the lineaments. The geotechnical data comes from the results of various geotechnical studies conducted by the Conakry Geoscience Agency.

2.2. Methods

The methodology adopted in this work consists of six steps: data acquisition—image processing—automatic extraction of lineaments—analysis and validation of lineaments—statistical and geostatistical analysis of lineaments—mapping of subsidence areas. It is based mainly on the use of USGS Landsat 8 imagery and geotechnical data. Researchers such as Sokeng et al. (2014), Jourda (2005), Anissa (2022), Montsion et al. (2021), Olasunkanmi et al. (2023) and Kamaraj et al. (2023b) used the same image acquisition methods for their study.

The combination of several spectral bands (false colors 7-6-4) in ArcGIS made it possible to create a composite image for detecting linear geological structures by emphasizing spectral and textural contrasts. This method is more effective than pixel by pixel analysis (Es-Sabbar Brahim, 2020; Kebede et al., 2021; Mwaniki et al., 2015; Magigita et al., 2023). One approach has been validated by the work of Fatma & Zahoua (2022). It uses the Image Analysis algorithm to generate GeoTIFF files highlighting linear structures associated with lineaments using infrared/red coupling. The Landsat 8 image, acquired under clear skies, did not require extensive atmospheric corrections. We therefore performed a visual check of its color composite directly in Google Earth. This was previously calibrated on the same date as the raw image acquisition date. From there, a visual comparison identified landscape discrepancies and general rendering imperfections. Several digital image processing techniques, including standard color composites, were used by Diédhiou et al. (2020) to map linear structures. The automatic detection algorithm in Geomatica was used to identify lineaments. Oludayo et al. (2021), Said (2024) and Ali & Oussama (2020), applied the same method to generate vector data, which was then validated and analyzed in GIS software. The validation, inspired by the methods of Kebede et al. (2021) and Gharmane et al. (2018), con-

sisted of a visual and systematic comparison of the detected lineaments with road and hydrographic networks and drilling data to verify their geological relevance in an urban context. The final results were exported to Excel and RockWorks 17 for statistical analysis, which consisted of characterizing the lineaments (length, orientation) using distribution laws. Geostatistics was used to view the spatial organization of the lineaments via a variogram adjusted to a theoretical experimental model. After converting the vector data (lineaments) into point data in ArcGIS 10.3, we used kriging for spatial interpolation of the data on a map background. The variogram model used made it possible to obtain a map showing areas of low mechanical strength (areas with high interstitial void density, areas favorable or unfavorable for water). These areas are where two or more lineaments intersect. The lineament results obtained are then superimposed on the geotechnical test data to locate areas at risk of subsidence in the municipality of Ratoma. The geotechnical parameters used for this purpose are water content, particle size distribution, and Atterberg limits. Grain size, in particular the fine particle content, is the important factor that directly influences the Atterberg limits of a soil, which in turn determines the soil's subsidence character (Gibbs, 1962; Jiménez Delgado & Guerrero, 2007; ASTM International, 2017; Tribak et al., 2020). The influence of particle size distribution on Atterberg limits can be explained by physicochemical principles related to the surface of the grains. These electrically charged sheet-like surfaces enable water molecules to be strongly adsorbed and retained. This interaction between water and fine particles gives the soil its cohesion and plasticity, explaining the high Atterberg limits (Ayadat & Ouali, 1999; NF EN ISO 17892-12, 2018; Douchet et al., 2017; Mamah et al., 2025).

The relationship used in this article to calculate the liquidity index is the one used in the work of ASTM International (2017). Based on soil mechanics research, we compared our results with the conditions of Feda (1966), which link the degree of saturation Sr0 of a soil to its liquidity index on the one hand, and its liquidity index to its settlement potential on the other. In 1966, Jaroslav Fedaalso proposed in his work a collapse index based on natural water content, degree of saturation, plasticity limit, and plasticity index. The definitive identification in this research is based on the liquidity index. The particle size distribution was interpreted by separating the pass and reject fractions using a 0.08 mm sieve.

Finally, a multi-criteria approach was used to map areas at risk of subsidence. The method is based on the Analytic Hierarchy Process (AHP) developed by Saaty in 1970 and Dar et al. (2010). This structured technique breaks down the problem into a hierarchy, allowing criteria to be compared and weighted in pairs (Bashe, 2017). The process includes identifying and developing decision criteria, classifying and standardizing criteria, and weighting and aggregating these criteria. This generates a summary map that facilitates informed decision-making. Despite the results obtained in this research, the use of only 11 samples for the entire municipality remains insufficient for reliable spatialization of ge-

otechnical information.

3. Results

3.1. Extraction and Mapping of Lineaments

Landsat 8, launched in 2013 by NASA and the USGS, is a satellite in the Landsat program designed for environmental monitoring, mapping, and natural resource management. It offers a spatial resolution of 15 m (panchromatic), 30 m (visible, NIR, SWIR), and 100 m (thermal). With a spectral resolution of 11 bands and a radiometric resolution of 16 bits, it allows for better distinction of spectral variations. Thanks to its radiometric depth and the program's historical archives, Landsat 8 is suitable for long-term studies. Landsat 8 products already undergo automatic geometric corrections by the USGS.

Automatic lineament extraction was performed using Geomatica. The configuration of the parameters (thresholding, contrast threshold, minimum length, and fileting) underwent three iterations in order to optimize the process and achieve the result shown in Figure 1.

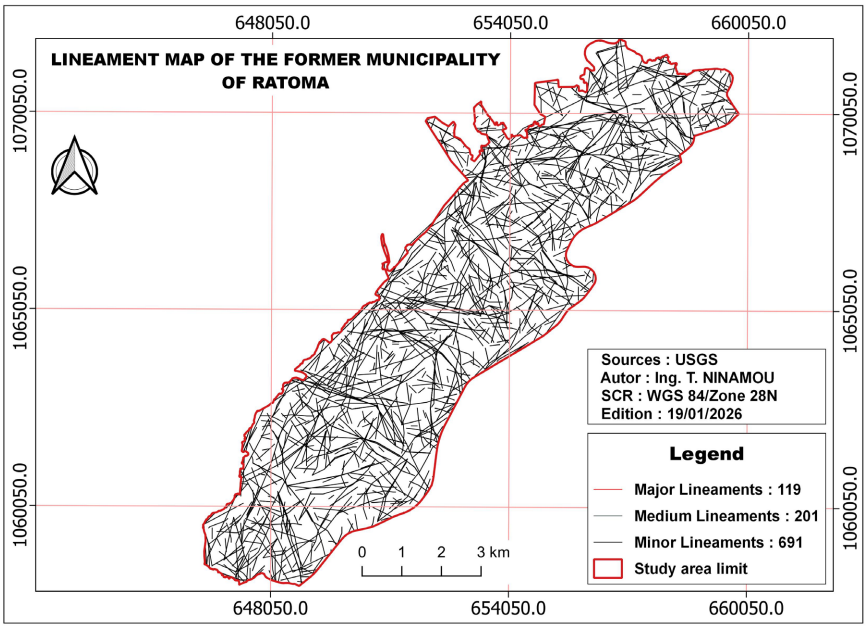

Figure 1. Mapping of lineaments in the study area.

3.2. Validation of the Lineaments in the Study Area

Validation consisted of superimposing the extracted lineaments on the hydrographic and road networks. Those that coincide with these surface features are selected and removed from the lineament network. Spatial analysis of the lineaments using high-yield drilling data reveals that all of these drill holes are located near a major lineament or in an area with a high density of lineaments, unlike low-yield drill holes, which are located further away.

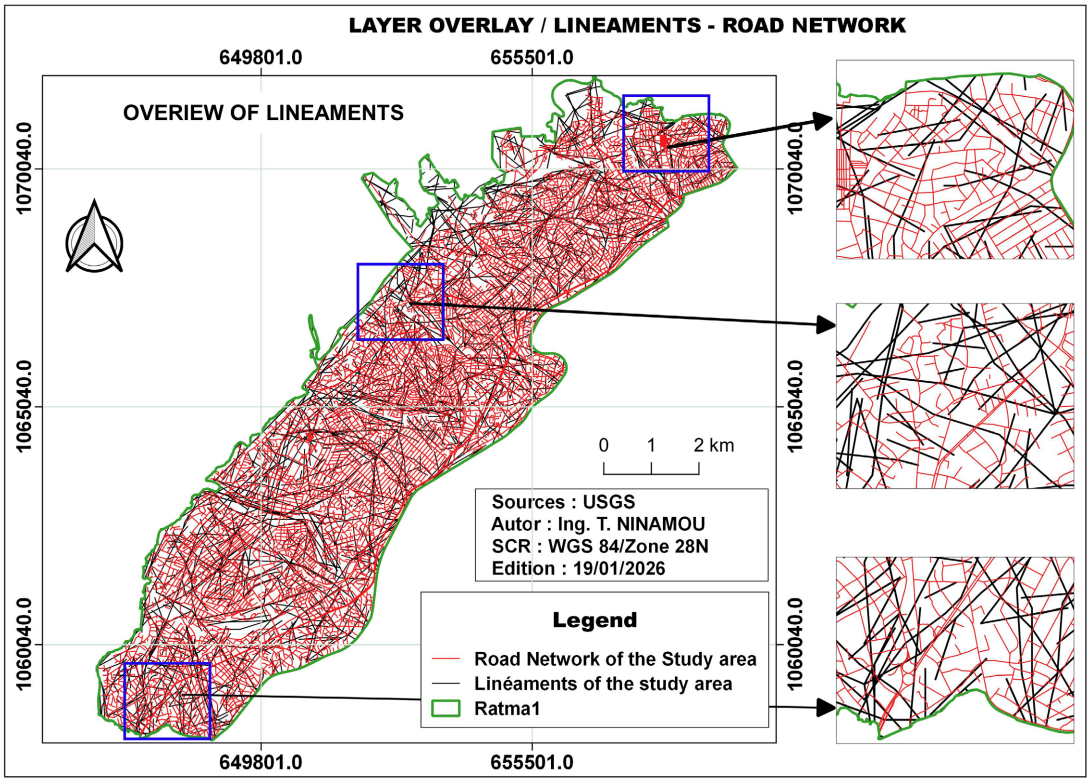

Figure 2. Validation of lineaments in relation to road networks in the study area.

3.3. Statistical Analysis, and Geostatistical Analysis of Lineaments

3.3.1. Statistical Analysis

Due to the complexity of the study area (urbanized area) and the objective of the study, the detailed map of lineaments obtained after various treatments shows high densities of lineaments of varying sizes. These lineaments vary from a few meters to less than 1 km for minor lineaments with a total length of 307,414.61 m, an average of 444.88 for a total number of 691; then from 1 to 2 km for medium-sized lineaments with a total length of 281,107.62 m, an average of 1398.55 for a total number of 201. Finally, the elements with a minimum length greater than 2 km are the major lineaments, with a total length of 359,256.62 m, an average length of 3018.96 m, and a total number of 119. This gives a total of 1011 lineaments, of which 68% are minor lineaments, 20% are medium lineaments, and 12% are major lineaments. The major lineaments include approximately 6% exceeding 5 km and 17% measuring between 3 and 5 km, while only 2 minor lineaments reach approximately 0,8 km. The longest lineament (17,715 km) crosses the study area from northwest to northeast. This characterization of lineaments is very important for geological and geomorphological analysis in order to assess their significance and spatial extent.

The fracture density map shown in Figure 3 expresses the number of lineaments per unit area. It reveals areas of high concentration (17.01 to 28.33 km/km^2) and low concentration (0 to 11.33 km/km^2) of lineaments in the study area.

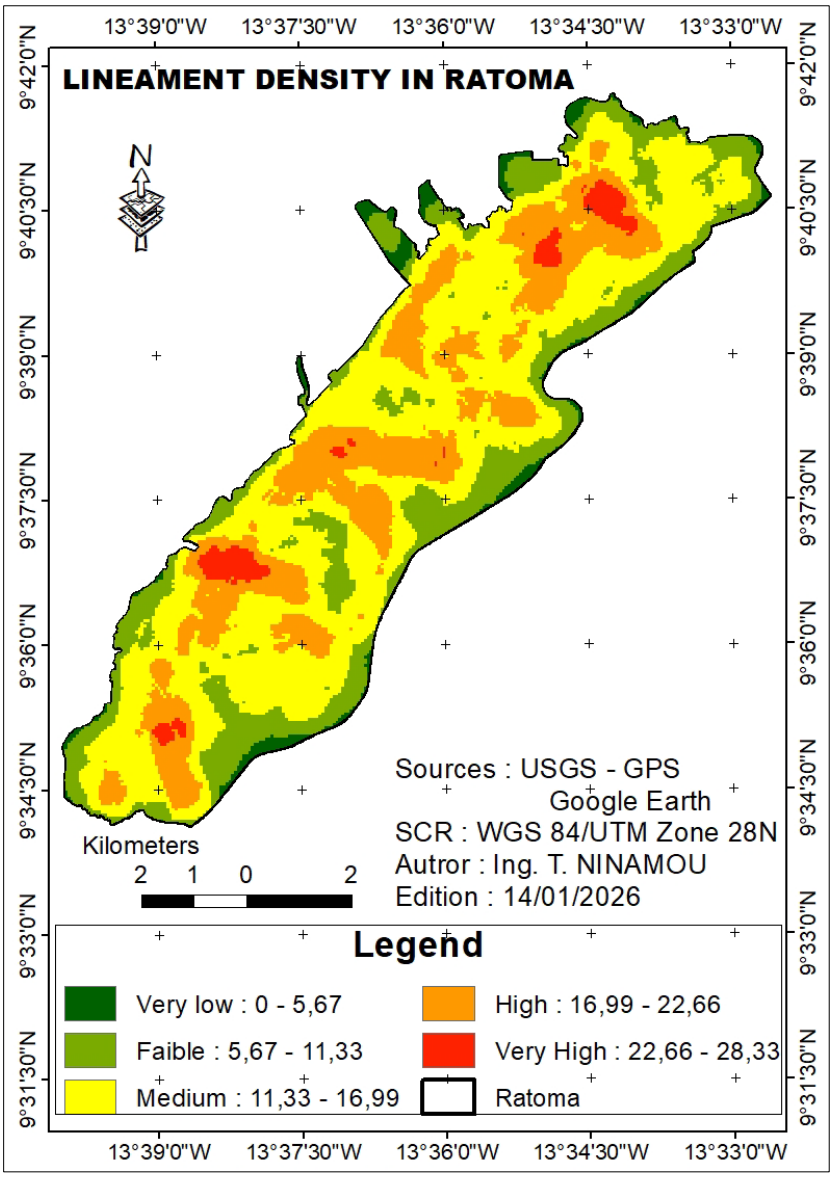

Figure 3. Map of the density of Ratoma lineam.

Figure 4 illustrates the interpolation variogram of underground lineaments, modeling fractures in all directions. The high values of this distribution of unstable areas represent 48.61% of the study area, while the low values represent 18.05%.

The orientation of the lineaments is analyzed by the rosettes illustrated in Figure 5. The lineaments are grouped into 12 orientation classes, based on angular intervals of 15˚. The distribution of fractures on the directional rosettes is relatively homogeneous for minor lineaments as shown in Figure 5(a), but irregular for major lineaments on Figure 5(c). However, all lineament families have frequencies exceeding 80%, with variations: 30% - 80% for minor lineaments, 16% - 80% for medium lineaments, and 8% - 83% for major lineaments. The layout of the lineament rosettes reveals two dominant orientation classes: NW-SE for major lineaments and NE-SW for medium lineaments. Each class also has a secondary

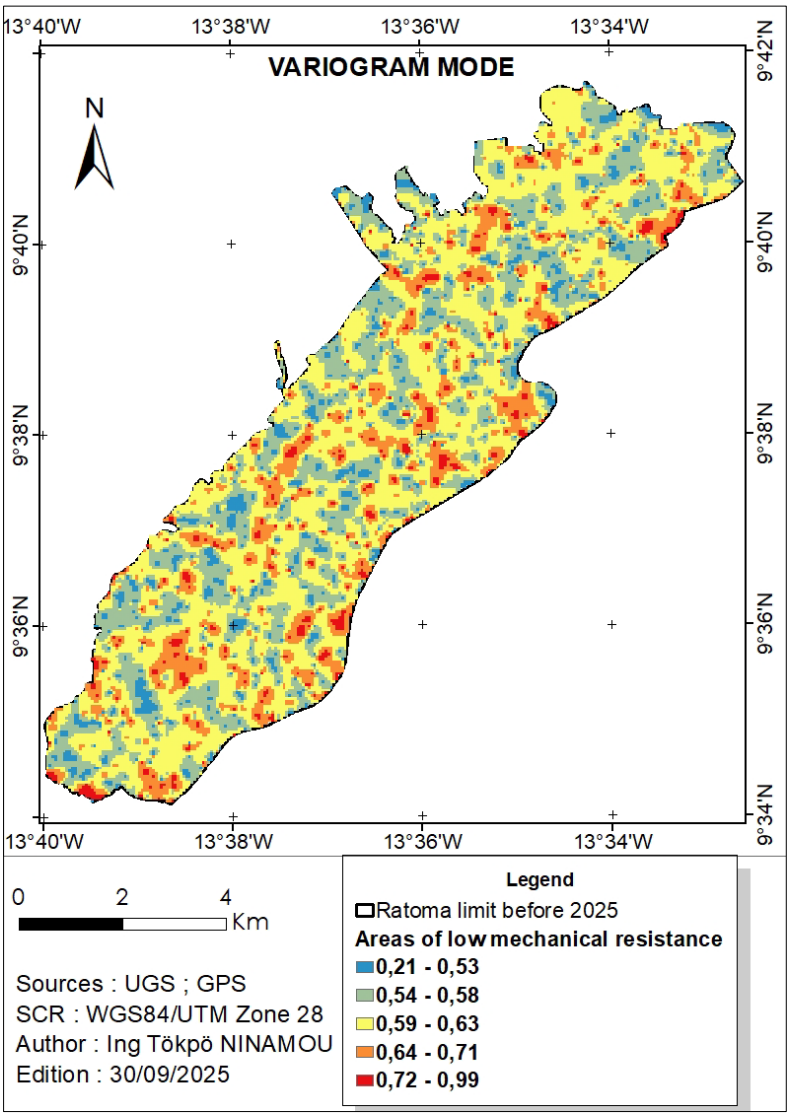

Figure 4. Map of the variogram model using kriging.

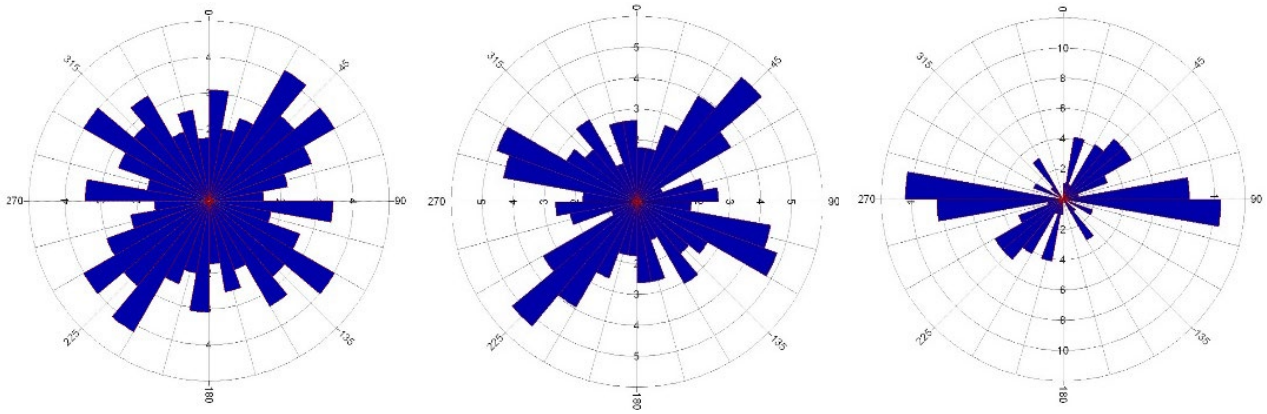

(a) (b) (c)

Figure 5. Diagram of directional rosettes. (a) Rosette of minor lineaments; (b) Rosette of medium-sized lineaments; (c) Rosette of major lineaments.

orientation, which is the opposite of the dominant one.

3.3.2. Geostatistical Analysis

Geostatistics is discussed here to show the spatial distribution of fractures and produce a model of fractured networks based on 2D cartographic analysis. Figure 4 shows the result of the geostatistical analysis of the lineaments. This map, which is the result of the spatial distribution of spherical experimental variograms, shows that the most fractured areas (those with low mechanical resistance) are scattered throughout the study area, with values ranging from 0.21 to 0.99. The map produced illustrates the distribution and spatial variability of these lineaments. It highlights geological discontinuities, such as groundwater circulation channels (lineaments) or shear zones. This spatial distribution shows the heterogeneity and extent of the lineaments, indicating a large-scale influence of linear geological structures.

Figure 4 (lineament density) and Figure 5 (void density), although different, complement each other. The first explains the geological behavior of linear structures, while the second characterizes their geotechnical properties. Both figures provide a comprehensive understanding of the phenomenon, incorporating both structural and mechanical factors affecting the soil. The synthesis of these two pieces of information is essential for a rigorous risk assessment and appropriate development planning.

3.4. Geotechnical Analysis of Soil Samples Taken at Ratoma

Table 1. Geotechnical characteristics of Ratoma soils.

Sample	Depth	Water content (%)	S_{r0} (%)	Grain size (%)		Atterberg limits		
				≥0.08	0.08≥	WL	WP	IP
EHamCon	3 to 5.6	25	60	73.9	26.1	42	27	15
Ekaporo	4 to 6	16.3	53	65	35	40	21	19
	8 to 9	23.5	72	40.7	59.3	38	17	21
Equipped1	1.5 to 3	17.6	57	45.1	30.8	40	26	14
Ekoloma	4 to 6	11.1	36	67.8	33.2	39	21	18
	7 to 10	12.9	33	44.2	55.8	39	16	23
Esonfon	6 to 7	18.2	46	43.1	58.9	38	19	19
	8 to 10	17.4	44	41.2	58.8	38	20	18
Equipped4	4 to 6	10.4	26	42.2	57.8	37	18	19
ENongTa1	3 to 4	26.6	68	61	39	44	25	19
ENongTa2	1.5 to 3	17.6	46	71.3	28.7	39	25	14
Esonforad	2.5 to 4	14.9	51.3	73.1	26.9	30	17	13
Ekobaya	5 to 7	15.5	57.6	65	35	38	19	19
Elamba	4 to 5	28.9	52.4	61.9	38.1	66	37	29
	6.5 to 7	48.3	93.8	44.2	55.8	48	24	24

Source: Conakry Geoscience Agency.

The comparison between the natural water content of a soil and its Atterberg limits provides an initial qualitative indication of its potential for settlement. Among the 11 samples analyzed in Table 1, only one (Elamba) has a natural water content almost equivalent to its liquidity limit (W = 48.3 and WL = 48) and a saturation degree close to 100%. This sample was taken at a depth of between 6.5 and 7 meters in the soil. The liquidity index (LI) is the indicator used to predict the behavior of a soil. LI is presented in Table 2.

Table 2. Identification of subsidence-prone areas in Ratoma.

Sample	Depth (m)	Liquidity index		Observation
		Calculated value	Reference value	
EHamCon	3 à 5.6	−0.13	IL < 0	Low risk of subsidence
Ekaporo	4 à 6	−0.25	IL < 0	Low risk of subsidence
	8 à 9	0.31	0 ≤ IL < 1	Moderate risk of subsidence
Ekipé1	1.5 à 3	−0.60	IL < 0	Low risk of subsidence
Ekoloma	4 à 6	−0.55	IL < 0	Low risk of subsidence
	7 à 10	−0.13	IL < 0	Low risk of subsidence
Esonfon	6 à 7	−0.04	IL < 0	Low risk of subsidence
	8 à 10	−0.14	IL < 0	Low risk of subsidence
Ekipé4	4 à 6	−0.40	IL < 0	Low risk of subsidence
ENongTa1	3 à 4	0.08	0 ≤ IL < 1	Moderate risk of subsidence
ENongTa2	1.5 à 3	−0.53	IL < 0	Low risk of subsidence
Esonforad	2.5 à 4	−0.16	IL < 0	Low risk of subsidence
Ekobaya	5 à 7	−0.18	IL < 0	Low risk of subsidence
Elamba	4 à 5	−0.28	IL < 0	Low risk of subsidence
	6.5 à 7	1.013	IL ≥ 1	Risk of significant subsidence

Table 2 shows that the Elamba sample has a liquidity index (LI) of 1.013 for a depth of 6.5 to 7 meters. This value, which is greater than or equal to 1, is consistent with the fact that its water content (W) is almost identical to its liquidity limit (WL). On the other hand, samples with an LI of less than 0, regardless of the depth at which they were taken, present a low risk of subsidence.

3.5. Mapping of Subsidence-Prone Areas in Ratoma

In this study, five criteria were used to identify areas at high risk of subsidence: slope, altitude, fracture density, mechanical resistance, and soil liquidity index. The combination of these topographical, geological, and geotechnical elements made it possible to create a map of susceptibility to subsidence, following the methodology described in the work of Ouattara et al. (2022).

The subsidence map shown in Figure 6 was produced by combining these five criteria, which are divided into three factors (topographical, geological, and geotechnical). It shows five classes with an uneven distribution.

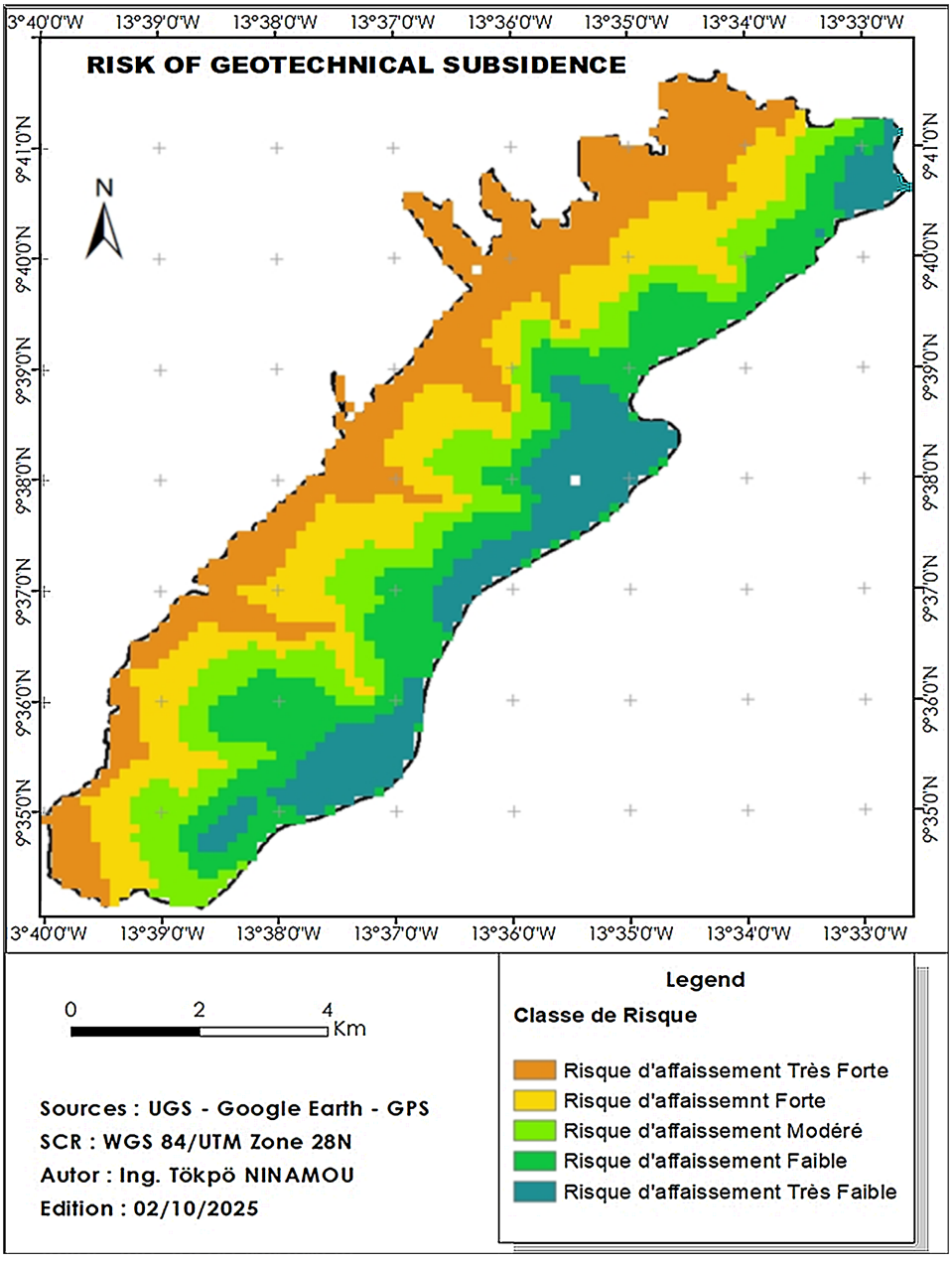

Figure 6. Map of areas at risk of subsidence.

The validation of the map of areas at risk of subsidence took into account the location of the 11 samples. The Lambanyi sample (Elamba, where IL > 1) confirmed its position, as did the Nongo Taady 1 sample (ENongTa1, where 0 ≤ IL < 1), which proved to be decisive. The final distribution indicates that 49.06% of the area is at risk of subsidence, 34.24% is at low risk, and 16.7% is at moderate risk. This categorization provides a clear representation of the vulnerability of the area.

4. Discussion

Remote sensing appears to be a fast and effective tool for identifying areas with geotechnical risks. It provides accurate and extensive data on surface and subsurface formations that may indicate the presence of fractured aquifers. Satellite and aerial imagery can be used to locate linear geological structures, identify depressions, and analyze the topography of the terrain (Gharmane et al., 2018). These depressions can be indicators of fractures or underground voids, which are important for groundwater circulation (Douchet et al., 2017). New methods for extracting linear features from satellite images were used in the work of Ali & Oussama (2020). Studies by Diédhiou et al. (2020) and Khallef et al. (2020) have also demonstrated the versatility of Landsat 8 data in various fields of remote sensing, ranging from geotechnical mapping to the analysis of land use changes and urban sprawl. For example, the work of El Aillah et al. (2019) highlighted the effectiveness of Landsat 8 for mining exploration by identifying lineaments and hydrothermal alterations in Morocco. In short, Landsat 8 is an important remote sensing tool, providing reliable data for numerous scientific and operational applications. The application of these studies in the context of this research, using the automatic lineament extraction method, yielded the result shown in **Figure 1**.

According to Ranjbari et al. (2023), combining different data sets during automatic feature extraction in Geomatica allows the optimal feature values to be determined. **Figure 2** illustrates the spatial distribution of the lineaments as well as the areas where the intersections between the lineaments are particularly pronounced. These areas correspond to the points of intersection of the lineaments. They could correspond to areas of low mechanical resistance in the subsoil consisting of voids through which groundwater can flow (Sokeng et al., 2014; Youan Ta et al., 2009). The main interest of the analysis of the lineament network is to find lineaments that are likely to represent areas of subsidence or shearing. This approach supports the objectives of the work in Solomon & Ghebreab (2006), which seeks to understand the nature and orientation of geological structures in order to determine their tectonic significance.

The method described in Scholz (2002), validated by field measurements and surveys, established a link between lineaments and fractures, making it possible to assess the stability of the terrain and locate the geological structures responsible for the disturbances. Thus, in this study, after validation of the lineaments, the results obtained revealed a predominance of short lineaments (68%), suggesting dense and localized fracturing. This corresponds to areas subject to diffuse tectonic stresses (Gharmane et al., 2018). However, major lineaments (longer than 2 km) could correspond to regional faults that have an impact on hydrogeology and soil stability (Rault, 2019). The work of Douchet et al. (2017) indicated that a high density of minor lineaments may reveal a weakened area prone to landslides, which would undermine soil stability. The study by Colbeaux & Sommé (1985) provides us with a theoretical basis for understanding the link between lineaments and risk areas.

For Ouattara et al. (2022), a homogeneous distribution of small lineaments may reflect polyphase fracturing. Furthermore, the preferential orientations of major lineaments may correspond to regional tectonic directions. This analysis is consistent with the direction of the longest lineament obtained in this study. It crosses the entire northern part of the municipality of Ratoma. It is the longest lineament in the study area (approximately 17 km oriented SE–NW) identified after the extraction of lineaments. Furthermore, the preferential orientation of the major lineaments corresponds to a southeast–northwest (SE–NW) direction, as shown in **Figures 5(a)-(c)**. For this reason, the major lineaments must be taken into account in regional development plans to avoid seismic or instability risks.

The diagrams in **Figure 5** show the dominant directions of the lineaments. This interpretation is important because, in most cases, groundwater tends to flow along the directions of fractures present in the rock. The work of Kebede et al. (2021) also addressed the analysis of lineaments using statistical methods.

To better understand the distribution of vulnerable areas, a kriging variogram model was developed to map areas with low mechanical resistance based on the lines. Analysis of **Figure 4** reveals the spatial distribution of these fragile areas. It is based on the work of Sokeng et al. (2014) and Jonathan et al. (2024), which highlights aspects of structural geology, rock mechanics, and geotechnical risk assessment.

The lineament density values shown in **Figure 6** correspond to the mechanical strength of the subsoil, which varies between 0.427 and 0.567. This figure shows heterogeneity in the spatial distribution of lineaments within the municipality of Ratoma. These low values suggest weakened areas, potentially associated with fractures, faults, or shear zones that could present geotechnical risks (landslides, slope instability). This hypothesis corroborates the results of Douchet et al. (2017).

From a geotechnical point of view, comparing the natural water content of soil samples with their Atterberg limits (**Table 1**) provides an initial qualitative indication of their potential for settlement or subsidence. Through the lineaments, water can moisten the soil by increasing its volume and then shrink as it dries, causing cracks and progressive deformation. If the reduction in the volume of the moistened soil during drying is sudden, the soil will subside. The Kiroti district is witnessing this phenomenon of subsidence in Conakry. The Lambanyi area presents a significant risk of settlement, as its water content is almost equivalent to the liquidity limit (NF EN ISO 17892-12, 2018; Opukumo et al., 2022; Ayadat & Ouali, 1999).

A comparative analysis of **Table 1** and **Table 2** shows that all samples with a saturation degree $S_{r0} \leq 60\%$ have a liquidity index $IL < 0$. According to Feda (1966), these types of samples have an apparent strength dominated by suction, where the grains rearrange themselves after a sudden disappearance of suction, causing volumetric settlement. Atterberg limits are essential tools in soil mechanics, allowing for qualitative and to a certain extent, quantitative prediction of the settlement of fine soils. They serve more as indicators of potential and mechanism than as direct measurements of the extent of settlement. According to the results

in Table 2, the sample with a liquidity index of approximately 1 is in a liquid state, which implies high compressibility and, consequently, a significant risk of settlement (Opukumo et al., 2022; Jiménez Delgado & Guerrero, 2007; Kebede et al., 2021; NF EN ISO 17892-12, 2018). This is because a subsiding soil is a specific type of compressible soil that suddenly loses its resistance.

In Ratoma, the combined use of remote sensing data, geotechnical data, statistical and geostatistical analysis, and the AHP approach provided important qualitative information on the spatial distribution of areas at risk of subsidence. The results indicate that the very high and high subsidence risk classes represent 49.06% of the area studied. The work in Hama Rash et al. (2024) demonstrated that the integration of spatial interpolation techniques, such as the geographically weighted regression (GWR) model, makes it possible to predict soil index properties in areas where geological structures are decisive. This includes water content and Atterberg limits. These methods thus improve the modeling and understanding of soil properties. The results in Figure 6 are directly related to specific physical parameters such as slope, fracture density, altitude, soil mechanical strength, and liquidity index. These elements are qualitative and quantitative indicators of geotechnical disorder within the subsoil. The AHP approach applied here was also used in the work of Hilali (2023) to characterize and evaluate soil quality based on several parameters.

5. Conclusion

Quantitative data (length, orientation) on lineaments are essential for risk mapping and sustainable water resource management. This study shows the vulnerability of the municipality of Ratoma, where urban growth and geological structure elements generate risks of subsidence. These risks are confirmed by past drilling failures and disturbances observed near the catchment sites (Kobayah and Nongo Stade).

Following this observation, a six-step methodological approach was applied to produce thematic maps. The coupling of lineament analysis with geotechnical data via the multi-criteria approach (AHP) enabled the identification of risk areas.

The study demonstrates the relevance of an integrated approach combining remote sensing, geostatistical analysis, and geotechnical data to assess the risk of subsidence in Ratoma, revealing that nearly half of the territory (49.06%) is at risk of subsidence. This strategy provides us with an essential decision-making tool for sustainable urban planning. This tool makes it possible to require geotechnical interventions in the most exposed areas to ensure the safety of populations and the sustainability of infrastructure.

Conflicts of Interest

The authors declare no conflicts of interest regarding the publication of this paper.

References

Ali, N., & Oussama, A., (2020). *Contribution of Remote Sensing (LANSAD 8 and ETM8*

images) to Geotechnical Mapping of the Souk-Ahras N.E. Algerien Region. Master's Thesis, Université Larbi Tébessi, Tébessa.

Anissa, M. (2022). *The Use of Multi-Band Imagery and Geographic Information Systems for Estimating and Mapping Soil Susceptibility to Water Erosion in Semi-Arid Areas, Case Study: Mellégue Watershed, Northeastern Algeria.* http://dspace.univ-setif.dz:8888/jspui/handle/123456789/4027

ASTM International (2017). *Standard Test Methods for Liquid Limit, Plastic Limit, and Plasticity Index of Soils (ASTM D4318-17e01).*

Ayadat, T., & Ouali, S. (1999). Identification des sols affaissables basée sur les limites d'Atterberg. *Revue Française de Géotechnique, No. 86,* 53-56. https://doi.org/10.1051/geotech/1999086053

Bashe, B. B. (2017). Groundwater Potential Mapping Using Remote Sensing and GIS in Rift Valley Lakes Basin, Weito Sub Basin, Ethiopia. *International Journal of Scientific Engineering and Research, 8,* 43-50.

Colbeaux, J., & Sommé, J. (1985). Signification des analyses de «linéaments» dans le nord de la France. *Hommes et Terres du Nord, 3,* 195-200. https://doi.org/10.3406/htn.1985.2000

Dar, I. A., Sankar, K., & Dar, M. A. (2010). Remote Sensing Technology and Geographic Information System Modeling: An Integrated Approach Towards the Mapping of Groundwater Potential Zones in Hardrock Terrain, Mamundiyar Basin. *Journal of Hydrology, 394,* 285-295. https://doi.org/10.1016/j.jhydrol.2010.08.022

Diédhiou, I., Mering, C., Sy, O., & Sané, T. (2020). *Mapping Land Use and Land Use Change through Remote Sensing* (p. 42). EchoGéo.

Doré, M. D. (2024). *Decentralization: Here Is the New Territorial Redistribution of the City of Conakry.* https://guineenews.org/2024/04/29/decentralisation-voici-le-nouveau-redecoupage-territorial-de-la-ville-de-conakry/

Douchet, G., Thiery, Y., Aubourg, C., Sénéchal, G., & Rousset, D. (2017). Analyse de grandes déformations de versants dans les Pyrénées: exemple de la moyenne vallée d'Ossau. *Communication aux Journées Aléas Gravitaires (JAG),* Besançon, 24-25 Octobre 2017, 1-7.

El Aillah, A., El Moriani, Z. E. A., & Souhassou, M. (2019). Use of Landsat 7 and 8 Multispectral Imagery for Mining Exploration: The Case of the Bou-Azzer-El Graara Buttonhole, Morocco. *International Journal of Innovation and Applied Studies, 28,* 17. http://www.ijias.issr-journals.org/

Embaby, A., Youssef, Y. M., & Abu El-Magd, S. A. (2024). Delineation of Lineaments for Groundwater Prospecting in Hard Rocks: Inferences from Remote Sensing and Geophysical Data. *Environmental Earth Sciences, 83,* Article No. 62. https://doi.org/10.1007/s12665-023-11389-x

Es-Sabbar Brahim, E. M. (2020). Lithological and Structural Lineament Mapping from Landsat 8 OLI Images in Ras Kammouna Arid Area (Eastern Anti-Atlas, Morocco). *Economic and Environmental Geology, 53,* 425-440.

Fatma, B., & Zahoua, H. (2022). *Remote Sensing Using Landsat-8 and Sentinel-2 Imagery in the Eglabs Region; Application of Geological Mapping of Sheets at 1:200,000 Gara Sayada, Kahel Morat, and Tilmsi Ould Haïda.* Mouloud Mammeri University. https://dspace.ummto.dz/handle/ummto/18987

Feda, J. (1966). Structural Stability of Subsident Loess Soil from Praha-Dejvice. *Engineering Geology, 1,* 201-219. https://doi.org/10.1016/0013-7952(66)90032-9

Fuladi, A. D., & Deshmukh, M. S. (2021). Lineament Mapping Using Remote Sensing and GIS Techniques in Part of WRC-1 Watershed, Chargarh River Basin, Central India. *Journal of Science and Technology, 6,* 172-182.

Gharmane, Y., Fartati, M. E., Amrani, S., & Hinaje, S. (2018). Mise À Jour De La Cartographie Géologique Et États Des Contraintes Tectoniques Dans La Zone De Bouchfâa (NW Du Massif De Tazekka, Maroc). *European Scientific Journal, ESJ, 14,* 193-205. https://doi.org/10.19044/esj.2018.v14n18p193

Gibbs, H. J. (1962). *A Study of Erosion and Tractive Force Characteristics in Relation to Soil Mechanics Properties.* U.S. Department of the Interior, Bureau of Reclamation.

Hama Rash, A. J., Khodakarami, L., Muhedin, D. A., Hamakareem, M. I., & Ali, H. F. H. (2024). Spatial Modeling of Geotechnical Soil Parameters: Integrating Ground-Based Data, RS Technique, Spatial Statistics and GWR Model. *Journal of Engineering Research, 12,* 75-85. https://doi.org/10.1016/j.jer.2023.10.026

Hilali, A. (2023). *Characterization and Evaluation of the Quality of Agricultural Soils Irrigated by Wastewater Drained by the Oued Day, Beni Mellal (Morocco).* Master's Thesis, Sultan Moulay Slimane University.

Jiménez Delgado, M. C., & Guerrero, I. C. (2007). The Selection of Soils for Unstabilised Earth Building: A Normative Review. *Construction and Building Materials, 21,* 237-251. https://doi.org/10.1016/j.conbuildmat.2005.08.006

Jonathan, M., Mjemah, I. C., Kimambo, O. N., & Hamad, A. A. (2024). A Geospatial Approach to Delineate Lineaments on the Granite Gneissic Terrain of Mpwapwa District, Dodoma, Central Tanzania. *Heliyon, 10,* e38346. https://doi.org/10.1016/j.heliyon.2024.e38346

Jourda, J. (2005). *Methodology for Applying Remote Sensing Techniques and Geographic Information Systems to the Study of Fissured Aquifers in West Africa. Concept of Spatial Hydrotechnics: The Case of Test Areas in Côte d'Ivoire.* Doctoral Thesis, University of Cocody.

Kamaraj, P., Jothimani, M., Panda, B., & Sabarathinam, C. (2023a). Improving Lineament Mapping Using RISAT-1 SAR Data, Nagpur and Surrounding Area in Central India. *Data in Brief, 52,* Article ID: 109939. https://doi.org/10.1016/j.dib.2023.109939

Kamaraj, P., Jothimani, M., Panda, B., & Sabarathinam, C. (2023b). Mapping of Groundwater Potential Zones by Integrating Remote Sensing, Geophysics, GIS, and AHP in a Hard Rock Terrain. *Urban Climate, 51,* Article ID: 101610. https://doi.org/10.1016/j.uclim.2023.101610

Kebede, H., Alemu, A., & Nedaw, D. (2021). Mapping Geologic Structures from Gravity and Digital Elevation Models in the Ziway-Shala Lakes Basin; Central Main Ethiopian Rift. *Heliyon, 7,* e08604. https://doi.org/10.1016/j.heliyon.2021.e08604

Khallef, B., Brahamia, K., & Oularbi, A. R. (2020). Application of Remote Sensing Indices to the Mapping of Urban Areas and Bare Soil: The Case of the City of Guelma (Northeastern Algeria). *International Journal of Innovation and Applied Studies, 28,* 452-457. http://www.ijias.issr-journals.org/

Magigita, M. M., Mshiu, E., & Mtelela, C. (2023). Application of Remote Sensing and Spectroradiometry in Geological Mapping: A Case Study of Handeni (QDS 148) Block, Eastern Mozambique Belt, Tanzania. *Tanzania Journal of Science, 49,* 1079-1096. https://doi.org/10.4314/tjs.v49i5.12

Mamah, I., Milanes, H. M., Wadia, K. D., & Bouamey, K. (2025). Geotechnical Characterization of Lime-Treated Clayey Sand, Usable in Pavement Layers in the Extreme Southwest of Togo. *Revue Internationale de la Recherche Scientifique (Revue-IRS), 3,* 16. http://www.revue-irs.com

Matar, P. M., Karifene, A., & Taisso, M. H. (2023). Lineaments as a Tool for Decision-Making in the Optimal Location of Boreholes in the Base Zone: Case of the Department of Abtouyour (Republic of Chad). *GSC Advanced Research and Reviews, 15,* 157-170. https://doi.org/10.30574/gscarr.2023.15.3.0191

Montsion, R. M., Perrouty, S., Lindsay, M. D., Jessell, M. W., & Frieman, B. M. (2021). Mapping Structural Complexity Using Geophysics: A New Geostatistical Approach Applied to Greenstone Belts of the Southern Superior Province, Canada. *Tectonophysics, 812,* Article ID: 228889. https://doi.org/10.1016/j.tecto.2021.228889

Mwaniki, M. W., Moeller, M. S., & Schellmann, G. (2015). A Comparison of Landsat 8 (OLI) and Landsat 7 (ETM+) in Mapping Geology and Visualising Lineaments: A Case Study of Central Region Kenya. *The International Archives of the Photogrammetry, Remote Sensing and Spatial Information Sciences, 7,* 897-903. https://doi.org/10.5194/isprsarchives-xl-7-w3-897-2015

NF EN ISO 17892-12 (2018). *Geotechnical Investigations and Testing—Laboratory Testing of Soils: Part 12: Determination of Liquidity and Plasticity Limits. Standard.*

Ninamou, T., & Diakité, S. (2021). Impact of the Proliferation of Boreholes on the Quantitative State of Groundwater in the Municipality of Ratoma—Conakry. *African Scientific Journal, 3,* 187-205.

Olasunkanmi, N. K., Magawata, U. Z., & Bayowa, O. G. (2023). Assessment of Image Ratio Technique: Targeting Structural Features and Mineralization Characteristics in the Southwestern Part of the Sokoto Basin in Nigeria Using Landsat 8 Imagery. *Kuwait Journal of Science, 50,* 803-811. https://doi.org/10.1016/j.kjs.2023.02.030

Oludayo, A. A., Chidi, O. V., & Kayode, O. F. (2021). Triangulation Approach for Mapping Groundwater Suitability Zones in Coastal Areas around Lagos, Nigeria. Using Multi-Criteria Decision-Making Technique. *NRIAG Journal of Astronomy and Geophysics, 10,* 423-442. https://doi.org/10.1080/20909977.2021.1987118

Opukumo, A. W., Davie, C. T., Glendinning, S., & Oborie, E. (2022). A Review of the Identification Methods and Types of Collapsible Soils. *Journal of Engineering and Applied Science, 69,* Article No. 17. https://doi.org/10.1186/s44147-021-00064-2

Ouattara, Z., Franck Emmanuel Gouédji, G., Ouattara, G., Olivier Kanga, K., Moro Boffoué, O., & Coulibaly, Y. (2022). Petro-structural Evaluation of the Toulepleu-Guéya Section on the Toulepleu-Ity Gold District, West Côte d'Ivoire. *Journal of Geosciences and Geomatics, 10,* 153-161. https://doi.org/10.12691/jgg-10-3-4

Ranjbari, M. R., Vagheei, R., & Salehi, H. (2023). Integration of Landsat-8 and Sentinel-1 Dataset to Extract Geological Lineaments in Complex Formations of Tepal Mountain Area, Shahrood, North Iran. *Advances in Space Research, 71,* 936-945. https://doi.org/10.1016/j.asr.2022.08.061

Rault, C. (2019). *Site Effects, Damage, and Slope Erosion in the Epicentral Zones of Active Mountain Ranges.* Earth Sciences.

Saaty, T. L. (1970). A Scaling Method for Priorities in Hierarchical Structures. *Journal of Mathematical Psychology, 15,* 234-281. https://doi.org/10.1016/0022-2496(77)90033-5

Said, L. A. M. K. (2024). Automatic Extraction of Structural Lineaments in the NADOR Region. *Revue de Géographie, No. 11-12,* 6. https://journals.imist.ma/index.php/Espaces/article/download/2258/1459/4037

Scholz, C. H. (2002) *The Mechanics of Earthquakes and Faulting* (2nd éd.). Cambridge University Press.

SEG (2009). *Campaign of 180 Hydraulic Drillings in Greater Conakry.* Study Report, SEG.

Sokeng, V. C. J., Kouamé, K. F., Ta, M. Y., Saley, M. B., & Kouamé, K. (2014). Automatic

Extraction of Lineaments from Satellite Images Using Neural Networks: Contribution to the Structural Mapping of the Precambrian Basement in the Bondoukou Region (Northeastern Côte d'Ivoire). *Revue Scientifique Internationale de Géomatique, 1,* 4-17.

Solomon, S., & Ghebreab, W. (2006). Lineament Characterization and Their Tectonic Significance Using Landsat TM Data and Field Studies in the Central Highlands of Eritrea. *Journal of African Earth Sciences, 46,* 371-378. https://doi.org/10.1016/j.jafrearsci.2006.06.007

Tribak, H., Belkacem, A., Garouani, A. E., & Lahrach, A. (2020). Etude Géotechnique des Sols Compressibles: Caractérisation, Mécanisme et Recommandation (Cas des Régions de Berrechid et Kenitra, Maroc). *European Scientific Journal ESJ, 16,* 321-336. https://doi.org/10.19044/esj.2020.v16n9p321

Yoshe, A. K. (2023). Groundwater Potential Zone Identification Using Remote-Sensing-based/Gis Based Machine and Analytical Hierarchy Process (AHP) for Abbay Watershed, East Africa. *Engineering Heritage Journal, 7,* 10-25. https://doi.org/10.26480/gwk.01.2023.10.25

Youan Ta, M., Lasm, T., Jourda, J. P., Kouamé, K. F., & Razack, M. (2009). Mapping of Geological Features Using Landsat-7 ETM+ Satellite Imagery and Analysis of Fracture Networks in the Precambrian Bedrock of the Bondoukou Region. *Remote Sensing Reviews, 8,* 119-135.